A Molecular Dynamics Study of Ionic Hydration Near a Platinum Surface

J. Seitz-Beywl, M. Poxleitner, and K. Heinzinger
Max-Planck-Institut für Chemie (Otto-Hahn-Institut), Mainz, Germany

Z. Naturforsch. **46a**, 876–886 (1991); received July 26, 1991

Two Molecular Dynamics simulations have been performed where a Pt(100) surface is covered with three layers of water molecules and a lithium or an iodide ion is placed additionally in the boundary layer. The flexible BJH model of water is employed in the simulations and the ion-water, platinum-water and platinum-ion potentials are derived from molecular orbital calculations. The simulations extended over 7.5 ps at an average temperature of 298 K. The effect of the Pt(100) surface on the ionic hydration is demonstrated by the comparison of the radial distribution functions, the orientation of the water molecules and their geometrical arrangement in the first hydration shells of the ions in the boundary layer with those in a 2.2 molal bulk LiI solution.

I. Introduction

The first simulation of an aqueous electrolyte solution at an interface was reported several years ago. Spohr and Heinzinger calculated various structural and dynamical properties of a 2.2 molal LiI solution between Lennard-Jones walls from a Molecular Dynamics (MD) simulation [1]. In the meantime the investigations of pure water near non-polar walls by computer simulations (see e.g. [2]) have been extended to water/metal interface. The description of the metal character of the walls by the image charge model had led to contradictions with experimental data and molecular orbital calculations [3]. For successful simulations of water at a Pt(100) [4–6] and a Pt(111) [7] surface it was necessary to introduce platinum-water potentials derived from molecular orbital calculations. In addition, it proved to be useful to employ the flexible BJH model of water [8] which had led to good agreement with experimental data as far as bulk electrolyte solutions were concerned [9]. Very recently also simulations were performed for water near charged Pt(100) surfaces [10].

On the basis of this experience it was now possible to extend the simulations to metal/electrolyte solution interfaces. In this paper two MD simulations are reported where a Pt(100) surface is covered by three layers of water molecules with either a lithium or an iodide ion additionally in the boundary layer. The platinum ion potentials have been derived from ab initio molecular orbital calculations [11]. The structure of the electrolyte solution in the boundary layer is described on the basis of density profiles, pair correlation functions and the orientation of the water molecules and their geometrical arrangement in the hydration shells of the ions. In addition, various energetic data are presented. The effect of the Pt surface on all these properties is evaluated by comparison with results from a newly performed simulation of a 2.2 molal bulk LiI solution.

Reprint requests to Dr. K. Heinzinger, Max-Planck-Institut für Chemie, Saarstr. 23, W-6500 Mainz, Germany.

II. Description of the Simulations

a) Interaction Potentials

The water-water interactions are described by a modified central force potential (BJH model) [8] which has proved its usefulness in simulations of various aqueous systems [9]. The platinum-platinum interactions are modeled by a harmonic nearest-neighbour potential [12] in order to enable the coupling between motions of the electrolyte solution and the lattice.

The interactions between water and the platinum (100) surface are described by a potential proposed by Spohr [4], based on extended Hückel molecular orbital calculations [13]. This potential leads to a preferred adsorption of the oxygen atom on top of a platinum atom with a lowest energy minimum of -37.5 kJ/mol. The platinum-Li^+ and platinum-I^- potentials are derived from molecular orbital calculations of one ion and a platinum cluster consisting of nine and five atoms, respectively. The potential energies of an Li^+ and I^- in the field of the infinitely extended platinum

0932-0784 / 91 / 1000-0876 $ 01.30/0. – Please order a reprint rather than making your own copy.

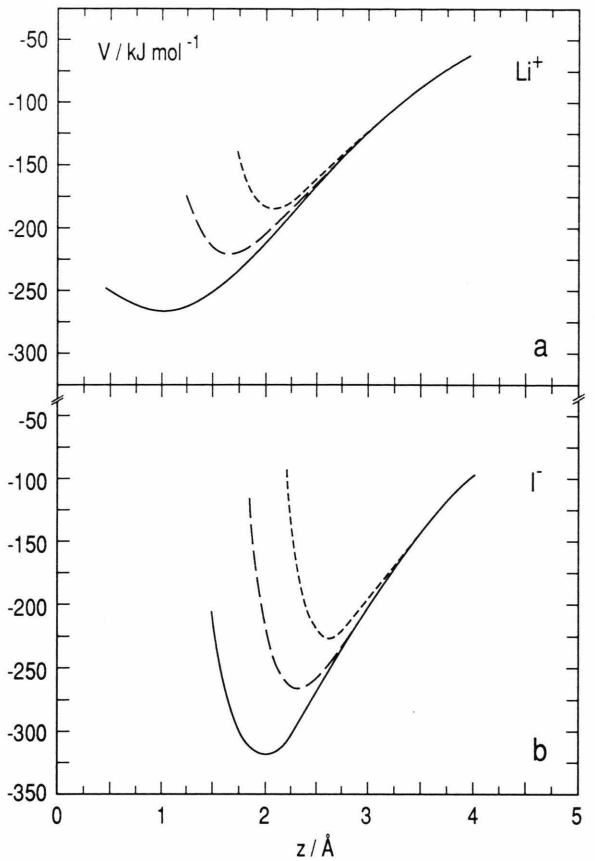

Fig. 1. Energies of Li^+ and I^- in the field of an infinite Pt(100) crystal, for ion positions on top of a platinum atom (– – –), on a bridge site (— —) and on a hollow site (——) [11].

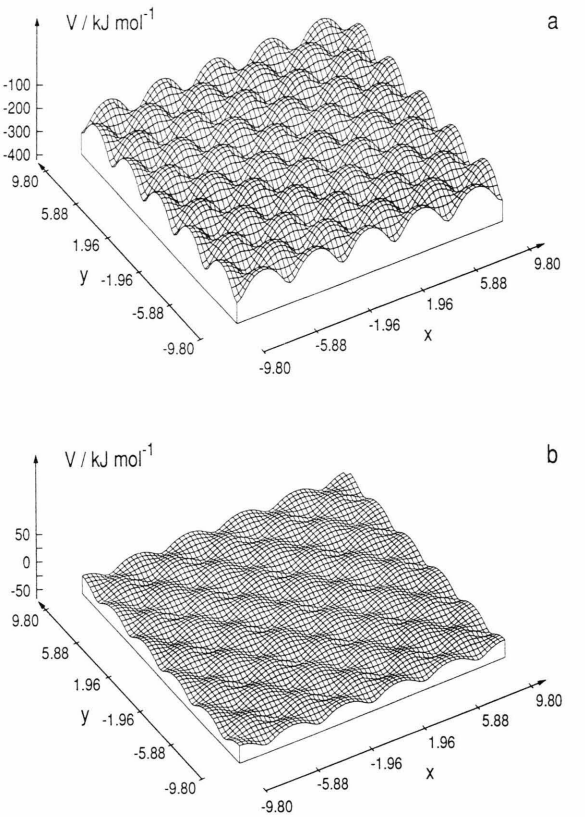

Fig. 2. I^--metal (a) and water-metal (b) interaction potentials as a function of x and y (in Å) for a distance z chosen in such a way that the potential has its minimum value. The dipole moment vector of the water molecule points away from the surface [4, 11].

crystal are shown in Fig. 1 as a function of surface-ion distance for the three cases where the ion is positioned on top of a platinum atom, on a bridge site (saddle site) and on a hollow site. The lowest minima amount to -265 and -319 kJ/mol for Li^+ and I^-, respectively, and are found for a hollow site configuration [11].

In Fig. 2 the potential energy of an iodide ion and a water molecule (with the dipole moment pointing away from the surface) in the field of an infinitely extended platinum crystal is presented as a function of the x- and y-coordinates of Figure 4a. The ion-surface and oxygen-surface distance z of Fig. 4b is chosen such that for each point (x, y) the potential has its minimum. The figure demonstrates clearly that the interactions employed in the simulation lead to a surface potential corrugation with deep minima in both cases [4, 11].

For further details of these potentials the reader is referred to the original publications cited.

Because of the high permittivity of the metal all charged particles in the liquid phase lead to induced charges in the platinum which will interact with all other charged particles in the solution. These many-body or surface-mediated interactions are described in the simulations by the image charge model and treated with the shifted force potential method [14].

A detailed investigation showed that these many-body interactions are only significant for very close distances between two ions and between an ion and a water molecule. As they are negligible for water-water interactions these many-body interactions have been neglected in the previous simulations of water/metal interfaces.

To certify consistency in the potentials, new ab initio calculations were performed also for the ion-water

Table 1. Parameters for the ion-water pair potentials according to Equation (1).

i	α	$Q_{i\alpha}$ [kJ Å mol^{-1}]	$A_{i\alpha}$ [kJ Å^2 mol^{-1}]	$B_{i\alpha}$ [kJ mol^{-1}]	$C_{i\alpha}$ [Å^{-1}]
Li	O	−917	−392	1.08×10^5	4.12
Li	H	458	146	1.13×10^4	5.50
I	O	917	265	2.30×10^5	2.90
I	H	−458	−147	2.29×10^7	6.27

interactions. The following analytical function was fitted to the energy points:

$$V(r) = Q/r + A/r^2 + B\exp(-Cr)\,. \qquad (1)$$

The parameters are given in Table 1. Figure 3 shows the Li^+-water and I^--water pair potentials as functions of the ion-oxygen distance for the water molecule orientations as shown in the insertion.

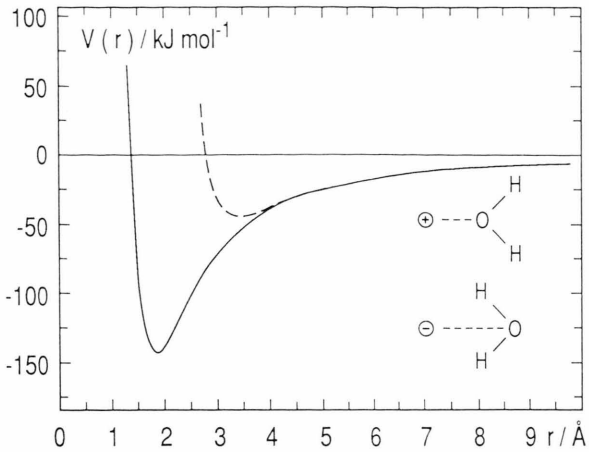

Fig. 3. Li^+-water (full) and I^--water (dashed) pair potentials as functions of ion-oxygen distance for the water molecule orientations shown in the insertions.

b) Details of the Simulations

For the simulations a rectangular basic box with side lengths $L_x = L_y = 19.6$ Å and $L_x = 25$ Å was used. The centers of the platinum atoms in the (100) face of the fcc platinum crystal lie in the (xy)-plane at $z = 0$. This plane is called the surface. In the range $-11.76 \le z \le 0$ seven layers are located, the seventh one being immobilized. The liquid phase reaches up to $z = 13.24$ Å, where a repulsive potential prevents an evaporation of the water molecules. Its position was choosen such that the density in the middle of the water phase was about 1 g/cm^3. Along the x- and y-directions periodic boundary conditions are introduced with a periodicity of L_x. This implies that the periodic platinum layers contain 50 atoms each, and the periodic upper rectangular prism contains 150 water molecules and one ion, Li^+ or I^-. So the system can be regarded as an infinitely extended slab with a thickness of 25 Å. Figure 4 shows two projections of the basic box.

In order to investigate the behaviour of ions near the platinum surface, one simulation was performed for each ion. The simulations were started with the ion positioned at about 2.5 Å distance from the surface. It remained in the boundary layer of water (1.5 Å $< z <$ 4.2 Å) over the whole simulation time, which extended – after an equilibrium period of 2.5 ps – over 30 000 time steps of 0.25 fs without rescaling. The average temperature was 298 K in both simulations. For the calculation of the Coulombic forces the two-dimensional Ewald summation was used [15], while the short-range interactions were treated with the shifted force method using a cutoff distance of $L_x/2$.

In order to elaborate the effect of the surface on the hydration of the ions, also a bulk simulation was performed introducing the new water-ion potentials. The basic periodic cube contained 200 water molecules and 8 ions of each kind, equivalent to a 2.2 molal LiI solution. The sidelength of the cube was 18.68 Å. The simulation extended over 15 000 time steps after equilibration without rescaling at an average temperature of 310 K.

III. Results and Discussions

a) Density Profiles

The normalized density profiles for the two ions, the oxygen and the hydrogen atoms as calculated from the two simulations are depicted in Figure 5. The positions and the heights in the O- and H-profiles are not significantly different from those for pure water at the Pt(100) surface [4]. The oxygen peak in the lithium simulation is slightly enhanced while in the iodide simulation this peak is reduced because of the excluded volume effect of the iodide. The ion profiles show that over the whole simulation time of 7.5 ps neither of the ions leaves the boundary layer.

The I^- profile extends only over the very narrow distance range $1.8 < z < 2.4$ Å. Its maximum at 2.0 Å coincides with the potential minimum for a position

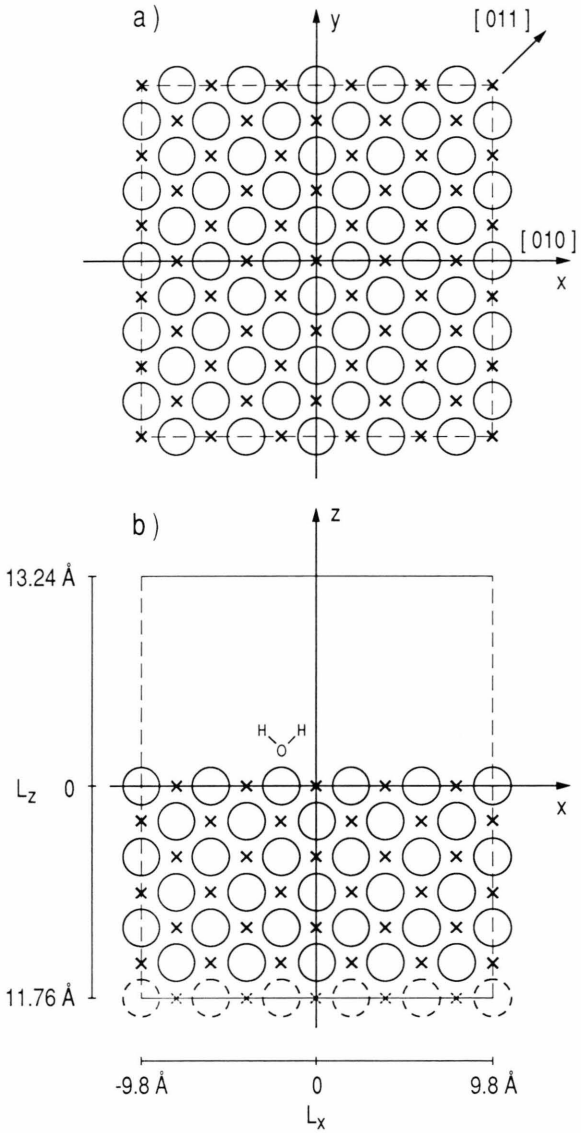

Fig. 4. (a) Sketch of the arrangement of the first (circles) and second (crosses) layer platinum atoms of the (100) surface coinciding with the $(x\,y)$ plane of the basic cell. The dashed lines are the periodic boundaries of the basic cell. The [010] and [011] directions of the crystal are indicated. (b) Corresponding sketch of the $(x\,z)$ plane. The three layers of water molecules and a Li^+ or I^- ion are located on top of the (100) face.

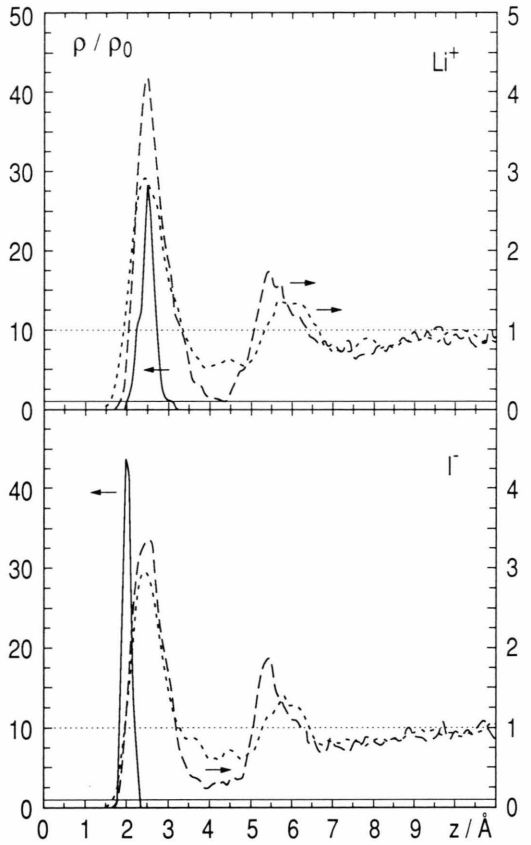

Fig. 5. Normalized ion, oxygen and hydrogen atom density profiles as functions of distance from the Pt(100) surface, calculated from simulations with a lithium ion and an iodide ion in the boundary layer. The curves are drawn for the ion (——), oxygen (— —) and hydrogen (– – –). The arrows refer to the corresponding scale.

of the iodide ion opposite of a hollow site of the Pt(100) surface (Figure 1). Therefore, the I^- can be called "contact adsorbed" on the Pt(100) surface, although the platinum crystal–iodide ion interaction energy is slightly less negative than the lowest potential minimum because the I^-–O first neighbour distance prevents the I^- from occupying an exact hollow site position.

The density profile of Li^+ is quite different from that of I^-. In spite of the smaller size of the lithium ion the range of distances from the surface $2.0 < z < 3.2$ Å is almost completely beyond that for the iodide ion and is much broader. The maxima of the O- and H-atom profiles coincide with that of Li^+ at 2.5 Å. It can be seen from Fig. 1 that at this distance the potential energy of Li^+ is independent of its position relative to the platinum atoms of the surface layer. It does not see a surface potential corrugation anymore. Very different from I^-, it is obvious that both the distance range of Li^+ from the surface and its position relative to the surface platinum atoms is determined by the Li^+-water and not by the Li^+–Pt

crystal interactions. Therefore, it is justified to say that the Li^+ is "not contact adsorbed".

The reason for the different behaviour of the two ions can be seen from Figure 3. The ion-water interaction energy is three times larger for Li^+ than I^-. The minimum in $V_{LiW}(r)$ appears slightly below 2 Å. This distance means that from an energetical point of view the Li^+ fits nicely into a hollow site of the quadratic water overlayer. Therefore, the first neighbour shell of Li^+ remains almost undisturbed – as far as the four water molecules in the boundary layer are concerned – which is not the case for I^- (see below).

b) Pair Correlation Functions

The radial pair distribution functions (RDFs) near the surface depend on z and converge for $z \to \infty$ towards those in the bulk. By taking averages of the RDFs over the z-ranges in which Li^+ and I^- moved during the simulations (see Fig. 5) we got RDFs of Li–O and Li–H for $\langle z_{Li} \rangle = 2.4$ Å and of I–O and I–H for $\langle z_I \rangle = 2.0$ Å. To take account of the excluded volume near the surface, the O- and H-densities around the ion were not related to a complete spherical volume but to a volume excluding the volume for which $z \leq 1.65$ Å. The running integration numbers are based on uncorrected RDFs in order to provide the correct number of neighbours.

Figure 6 shows the Li–O and Li–H RDFs for $\langle z_{Li} \rangle = 2.4$ Å and for the bulk of a 2.2 molal LiI solution. The first and second peaks in $g_{LiO}(r)$ and $g_{LiH}(r)$ are significantly more pronounced in the boundary layer and a far ranging order exists, which extends even beyond 9 Å. In the bulk solution both RDFs become uniform already beyond about 5 Å. Different from the Li-water RDFs the first peaks in $g_{IO}(r)$ and $g_{IH}(r)$ are slightly less pronounced but the far ranging order remains, as can be seen from Figure 7.

The reason for this enhancement of the hydration shell structure of Li^+ and the slight decrease for I^- in the surface layer results from the formation of a pronounced quadratic water overlap with a lattice constant of the Pt(100) surface of 2.77 Å.

In Fig. 8 the origin ($\Delta x = 0$, $\Delta y = 0$) coincides with the changing position of an O, a Li^+ or a I^- particle in the surface layer ($z < 4.2$ Å), and $|\Delta x|$ and $|\Delta y|$ are the absolute values of the projection of the distances of O-atoms in the surface layer from these reference particles. Both the reference particle and the O-atoms

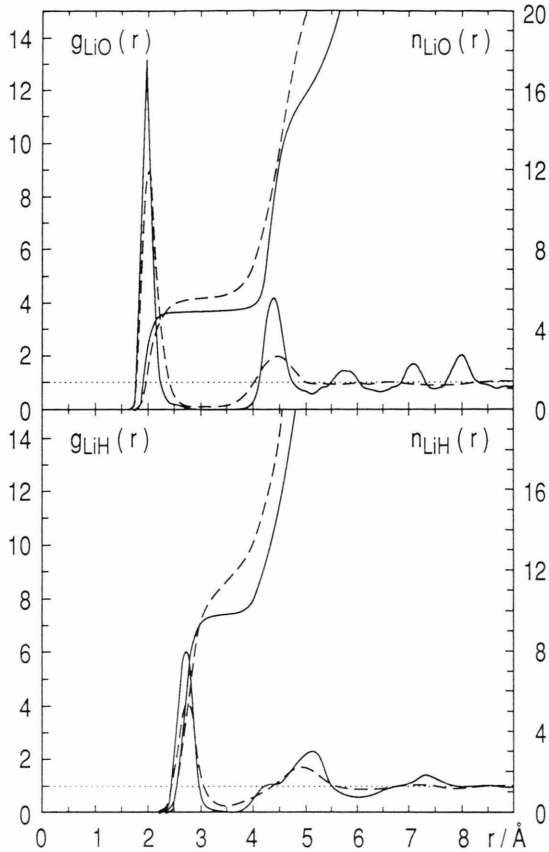

Fig. 6. Corrected lithium-oxygen and lithium-hydrogen radial distribution functions and the number of neighbours for the lithium ion in the surface layer at 2.4 Å (full) and in the 2.2 molal bulk LiI solution (dashed).

referred to move with respect to the Pt-lattice, and the shape of the peaks results from both movements.

The plot of g_{OO} reflects the positions of the oxygen atoms on the top site of the platinum lattice, and the pregnant form of the peaks refers to their relatively small displacement. The sharper peaks for g_{LiO} show that the displacements of Li^+ at its hollow site are smaller than those of O at its top, and the significantly broader ones for g_{IO} than for g_{OO} show that the displacements of I^- are much larger than those of O. Indeed the I^- moves in a relatively widespreaded area between a hollow and a bridge site.

In Fig. 9 the trajectories of Li^+ (a) and I^- (b) are drawn and the x- and y-coordinates of the oxygen atoms of the water molecules with $z < 4.2$ Å are marked by a dot after every 0.05 ps. The positions of those Pt atoms are not covered by oxygen atoms are indicated by crosses.

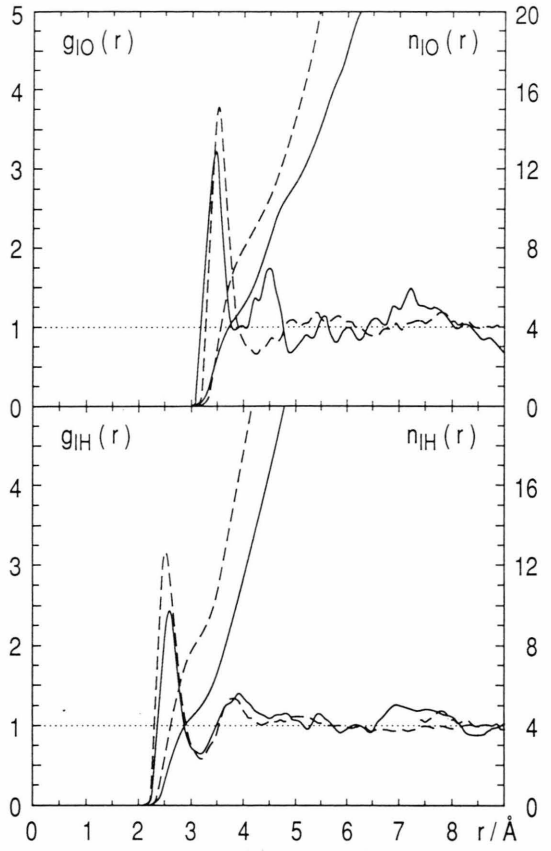

Fig. 7. Corrected iodide-oxygen and iodide-hydrogen radial distribution functions and the number of neighbours for the iodide ion in the surface layer at 2.0 Å (full) and in the 2.2 molal bulk LiI solution (dashed).

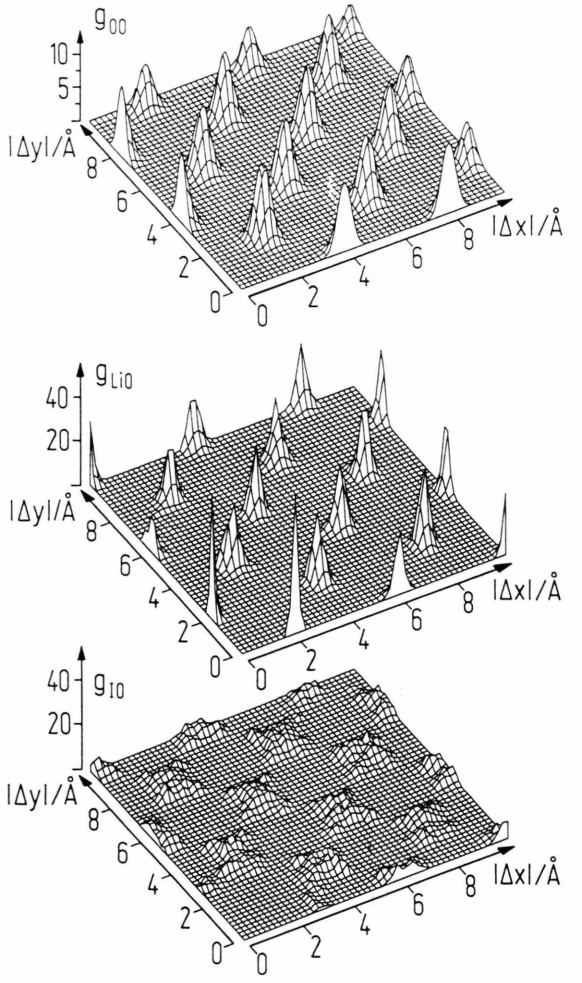

Fig. 8. Oxygen-oxygen, lithium-oxygen and iodide-oxygen pair correlation functions in the adsorbed layer ($z \leq 4.2$ Å for all particles).

Over the whole simulation time of 7.5 ps the Li^+ remains very near to the hollow site of the Pt(100) surface at $x, y = 1$ (Figure 9a). In accordance with Fig. 8 the distributions of the neighbouring oxygen atoms above their respective Pt atoms is very narrow. There is one surface Pt atom ($x = -3$; $y = -5$) with no oxygen atom in its neighbourhood. Only one oxygen atom seems to move in this this time period to another Pt atom.

The larger I^- moves during the 7.5 ps in the area $-4.0 < x < -2.5$ and $0 < x < -2.5$ and $0 < y < 1.0$ Å. It cannot occupy a hollow site as the first neighbour $I^- - O$ distance is about 3.4 Å. In accordance with the energy curves in Fig. 1 it prefers positions between a hollow site and a bridge site, where iodide-water and platinum-water binding energy is gained by only a small loss of the iodide-platinum one relative to the hollow site position. Necessarily, two of the four neighbouring Pt atoms are not covered by oxygen atoms and their distributions around the other Pt atoms are broader than in the Li^+ case.

c) Hydration Shell Symmetries

Besides the ion-oxygen and ion-hydrogen RDFs, in Figs. 6 and 7 the corresponding running integration numbers are presented which are defined by

$$n_{ij}(r) = 4\pi \varrho_0 \int_0^r g_{ij}(r')\, r'^2\, \mathrm{d}r' , \qquad (2)$$

where ϱ_0 is the average number density of the particles of kind j. The hydration number of an ion is usually

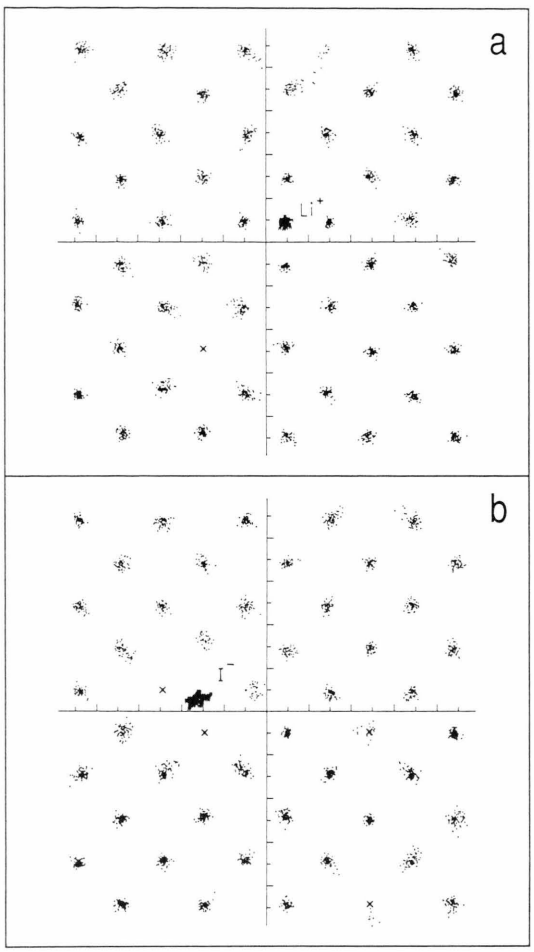

Fig. 9. Distribution of the oxygen atoms together with the trajectory of the lithium ion (a) and the iodide ion (b) in the (x, y) plane (Figure 4a). Only the oxygen atoms with a distance from the surface $z < 4.2$ Å are included and their positions are marked by dots in intervals of 0.05 ps. The platinum atoms of the surface layer which are not covered by oxygen atoms are marked by crosses.

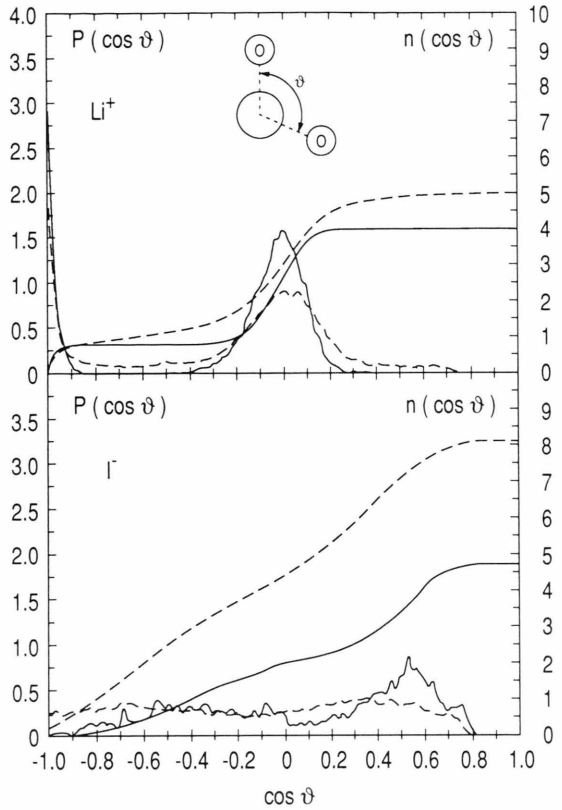

Fig. 10. Distribution of $\cos \vartheta$ – where ϑ is defined in the insertion – for the water molecules in the first hydration shells of Li^+ and I^- in the boundary layer (full) and the 2.2 molal bulk solution (dashed). The corresponding running integration numbers are shown additionally.

defined as $n_{\mathrm{IonO}}(r_{\mathrm{m1}})$ where r_{m1} stands for the position of the first minimum in the ion-oxygen RDF. With this definition the hydration numbers for the lithium (iodide) ion in the bulk solution and this in the boundary layer are found to be 5.8 (9.2) and 4.9 (5.1), respectively. Obviously the smaller values in the boundary layer result from the excluded volume effect of the Pt surface.

The geometrical arrangement of the oxygen atoms in the first hydration shells of the ions can be deduced from the simulation by the calculation of the distribution of $\cos \vartheta$, where ϑ is defined as the O–Ion–O angle. The result is depicted in Fig. 10 for both ions in the boundary layer and in the bulk solution. The corresponding running integration numbers for $\cos \vartheta$ are shown additionally.

The distribution of $\cos \vartheta$ for Li^+ demonstrates clearly a strong preference for an octahedral symmetry in both cases. $P(\cos \vartheta)$ is narrower around 0 and -1 for the boundary layer in accordance with the sharper first peaks in the Li–O RDF (Fig. 6) and the well-defined nearest neighbour oxygen atom positions of Li^+ in the quadratic water overlayer (Figs. 8 and 9). The hydration number of Li^+ is reduced by about one in the boundary layer. As the octahedral plane of the hydration shell of Li^+ parallel to the surface is fully occupied, the excluded volume of the surface is responsible for the missing water molecule. The fifth water molecule belongs to the second water layer and is placed on top of the ion. In this way the ratio of the number of oxygen atom neighbours in the first hydration shell with $\vartheta = 90°$ to those with $\vartheta = 180°$, which

is 4 in the bulk solution, remains the same in the boundary layer.

It can also be seen from Fig. 10 that neither in the bulk nor in the boundary layer a symmetry is recognizeable for the hydration shells of I^-. $P(\cos \vartheta)$ is practically uniform over he whole range except for the excluded volume effect for $\cos \vartheta > 0.8$ which results from the finite size of the water molecules. As the I^- is contact adsorbed the excluded volume effect of the Pt surface amounts to almost one half and is responsible for the reduction of the hydration number of I^- from 9.2 in the bulk solution to 5.1 in the boundary layer.

d) Orientation of the Water Molecules

The orientations of the water molecules in the first hydration shells of Li^+ and I^- are described by the distribution of $\cos \Theta$, where Θ is defined as the angle between the dipole moment direction of the water molecule and the vector pointing from the oxygen atom towards the center of the ion. The distributions for Li^+ and I^- in the boundary layer are compared in Fig. 11 with those for the bulk LiI solution. $P(\cos \Theta)$ for Li^+ shows in both curves a strong preference for a anti-dipole moment orientation. The distribution is narrower for the boundary layer in accordance with the significantly more pronounced first hydration shell as discussed above.

The most significant difference between the newly performed simulation of the 2.2 molal LiI solution with the BJH model for water and the former one, where the ST2 model for water was employed [16], exists for $P(\cos \Theta)$ for Li^+. From the former simulation the maximum of the distribution was found for $\cos \Theta \approx 0.6$, which means that a lone pair orbital of the water molecule is directed towards the Li^+. The new results are expected to be much more reliable than the former ones as in the ST2 model the directionality of the lone pair orbitals seems to be exaggerated by the negative point charges.

Both distributions of $\cos \Theta$ for I^- are very broad. The positions of the maxima indicate a preference for an angle Θ between a linear hydrogen bond formation (which was found for the chloride ion from simulations of various alkaline earth chloride solutions [17]) and an orientation where the dipole moment vector of the water molecule is directed towards I^-. The shift of the maximum in $P(\cos \Theta)$ in the boundary layer means a decrease of 10° relative to the preferential

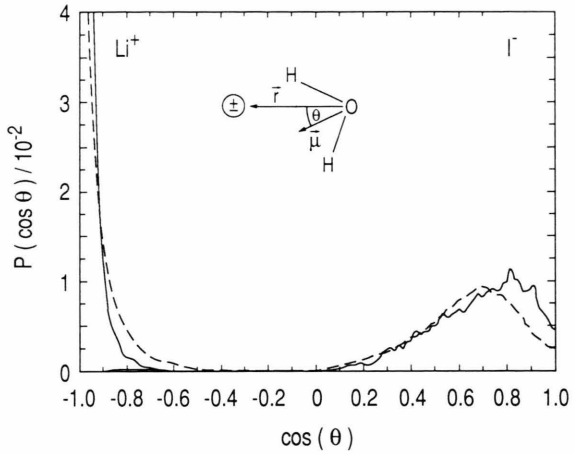

Fig. 11. Distribution of $\cos \Theta$ – where Θ is defined in the insertion – for the water molecules in the first hydration shells of Li^+ and I^- calculated from the simulations with the ion in the boundary layer (full) and in a 2.2 molal bulk LiI solution (dashed).

value of Θ in the bulk solution. The quadratic water overlayer which still exists even in the neighbourhood of I^- (Fig. 9 b), is responsible for this shift.

The average value of $\cos \Theta$ as a function of ion-oxygen distance is depicted in Fig. 12 for Li^+ and I^- in the boundary layer and in the bulk LiI solution. In order to demonstrate more clearly the effect of the hydrogen bonding in the quadratic water overlayer on $\langle \cos \Theta(r) \rangle$, only the water molecules in the surface layer ($z < 4.2$ Å) are included in the averaging procedure.

In accordance with Fig. 11 in both cases $\langle \cos \Theta(r) \rangle \approx -1$ over the whole range of the first hydration shell of Li^+. There is also agreement between boundary layer and bulk solution for the second neighbour shell. As in the surface layer the Li–O distance distribution is not continuous, different from the bulk case the $\langle \cos \Theta(r) \rangle$ curve is discontinued between the first and second shell. While beyond the second shell the average value of $\cos \Theta$ in the bulk solution decreases rapidly to values near zero, $\langle \cos \Theta(r) \rangle$ changes sign in subsequent distance ranges of the surface layer. The rather large absolute values of $\langle \cos \Theta(r) \rangle$ in the different distance ranges indicate strong correlations between distance and orientation in the boundary layer. It is obvious from Fig. 11 that for distances beyond 5 Å the orientation of the water molecules is mainly determined by the structure of the water overlayer.

The broad distributions of $\cos \Theta$ for the first hydration shells of I^- in Fig. 11 are reflected in the average

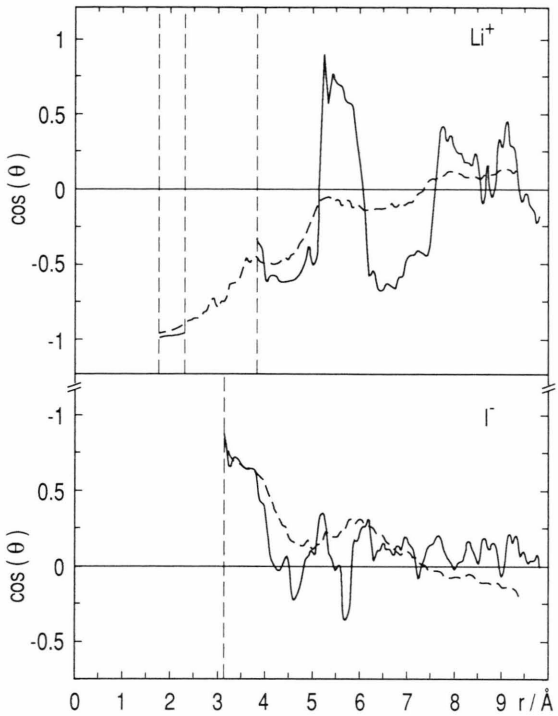

Fig. 12. Average value of cos Θ as a function of ion-oxygen distance calculated from simulations with Li^+ and I^- in the boundary layer (full) and in a 2.2 molal bulk LiI solution (dashed). The vertical lines mark the area where no water molecules are found.

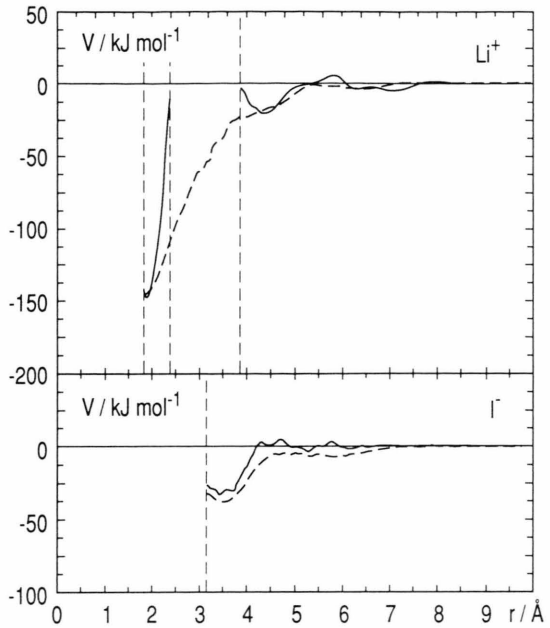

Fig. 13. Average potential energy of a water molecule in the field of a lithium and an iodide ion from simulations with the ion in the boundary layer (full) and in the bulk solution (dashed). Only the water molecules in the surface layer ($z < 4.2$ Å) are included in the calculation of the full curve. The vertical lines mark the area where no water molecules are found.

values of about 0.7 in both cases. The rapid decrease of the preferential orientation with distance even for the boundary layer is a consequence of the larger area covered by the I^- trajectory and the broader distributions of the oxygen atom positions around the platinum atoms of the (100) surface when compared with the Li^+ case (Figure 9).

e) Average Potential Energies and Pair Interaction Energy Distributions

The average potential energies of the water molecules in the fields of the Li^+ and the I^- as a function of ion-oxygen distance are presented in Fig. 13 for the ions in the bulk solution and in the boundary layer. In the latter case again only the water molecules in the surface layer ($z < 4.2$ Å) are included in the averaging in order to clarify the effect of the wall. The positions and the depth of the first minima coincide with those of the ion-water pair potentials for the most favourable orientations.

For both ions the average potential energies reflect the orientational behaviour of the water molecules. For Li^+ negative values of $\langle \cos \Theta(r) \rangle$ correspond to negative average potential energies and vice versa. It is the other way around in the case of I^-. For a given orientation the absolute value of the energy decreases with $1/r^2$ for distances beyond about 4 Å.

The normalized ion-water pair interaction energy distributions are presented in Fig. 14 for Li^+ and I^- in the bulk solution and in the boundary layer. In the latter case again only the water molecules in the surface layer ($z < 4.2$ Å) are included in the distribution.

The first and second hydration shell of Li^+ can be recognized in Fig. 14 also from an energetical point of view for the bulk solution and the boundary layer. The peak on the positive energy side at about 18 kJ/mol is found only in the boundary layer. It reflects the positive energies in $V_{LiW}(r)$ in the range between 5 and 6 Å (Fig. 13) which in turn are a consequence of the energetically unfavourable orientations as depicted in Figure 12. If the water molecules in the second and third

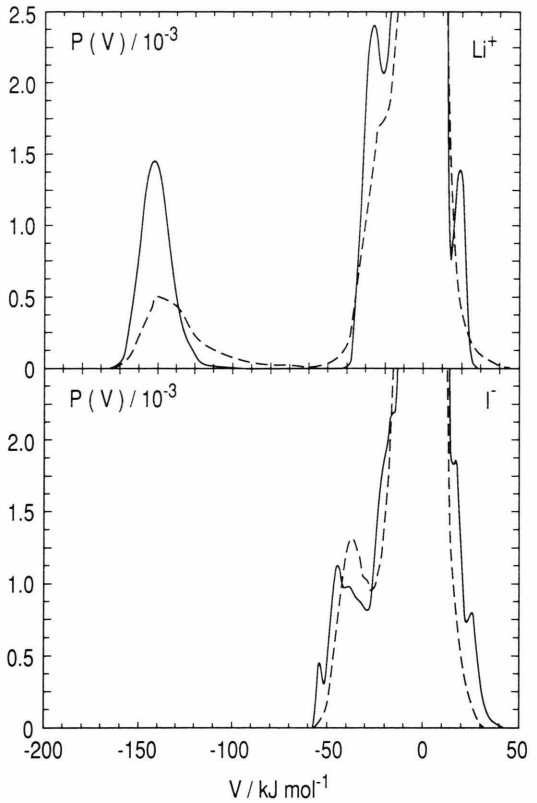

Fig. 14. Normalized ion-water pair interaction energy distributions for Li^+ and I^- in the boundary layer (full) and in the bulk solution (dashed). Only the water molecules in the surface layer are included in the calculation of the full curve.

water layer would have been included in this distribution the effect of the surface would have become less clear. A much smoother curve would have resulted.

The hydration shell of I^-, which is reflected energetically by a single peak in the bulk solution, shows two maxima for the boundary layer. This splitting of the peak follows from the size of the I^- which prevents that more than two neighbouring Pt atoms of the (100) surface are covered by oxygen atoms as discussed above (Figure 9). Thus considering only the surface layer the first neighbour shell of I^- consists of two parts with only two water molecules as first neighbours. This geometrical picture is reflected here energetically. On the positive energy side the shoulders reflect again energetically unfavourable orientations of the water molecules relative to the I^- (Figs. 12 and 13).

V. Summary

For the hydration shell of the lithium ion in the boundary layer a well defined octahedral structure is found slightly more pronounced than that in the bulk solution but with the exception that one water molecule of the octahedron is replaced by the platinum wall. As the Li^+-water interactions prevail, the ion is kept within the first water layer, which means far away from the Li^+–Pt crystal potential minimum. Therefore, the lithium ion should not be called contact adsorbed, although there is no water molecule between the ion and the platinum surface.

In contrast to Li^+ the size of the I^- leads to a competition between the tendency of the water molecules to preserve the quadratic overlayer and that of the I^- to occupy a hollow site position. The hydration shell structure in the surface layer resulting from this competition is such that the iodide ion occupies a position between a hollow and a bridge site of the Pt(100) surface and all platinum atoms except the two nearest to the I^- are covered by the oxygen atoms of the water molecules. In this way the ion can approach the surface up to the distance where it reaches almost the lowest I^-–Pt crystal potential energy. Therefore, the iodide ion can be called contact adsorbed.

In this paper for the first time MD simulations are reported on the complicated system consisting of a metal wall, water molecules and ions. The consistency of the results seems to prove the feasibility of such simulations and the ability to provide – at least qualitative – information on a molecular level which is up to date neither available from experiments nor from analytical theory. Although there are undoubtedly ample changes to improve the potentials employed and various details of the simulation, the experience collected in this investigation encourages the extension of this kind of simulations.

Acknowledgement

Financial support by Deutsche Forschungsgemeinschaft is gratefully acknowledged.

[1] E. Spohr and K. Heinzinger, J. Chem. Phys. **84,** 2304 (1986).
[2] E. Spohr and K. Heinzinger, Electrochim. Acta **33,** 1211 (1988).
[3] K. Heinzinger and E. Spohr, Electrochim. Acta **34,** 1849 (1989).
[4] E. Spohr, J. Phys. Chem. **93,** 6171 (1989).
[5] E. Spohr, Chem. Phys. **141,** 87 (1990).
[6] K. Foster, K. Raghavan, and M. Berkowitz, Chem. Phys. Lett. **162,** 32 (1989).
[7] K. Raghavan, K. Foster, K. Motakabbir, and M. Berkowitz, J. Chem. Phys. **94,** 2110 (1991).
[8] P. Bopp, G. Janscó, and K. Heinzinger, Chem. Phys. Lett. **98,** 129 (1983).
[9] K. Heinzinger, in: Computer Modelling of Fluids, Polymers, and Solids (C. R. A. Catlow, S. C. Parker, and M. P. Allen, eds.), Kluwer Academic Publishers, Dordrecht 1990, p. 357.
[10] G. Nagy and K. Heinzinger, J. Electroanal. Chem. **296,** 549 (1990).
[11] J. Seitz-Beywl, M. Poxleitner, M. Probst, and K. Heinzinger, Int. J. Quantum Chem., in press.
[12] J. E. Black and P. Bopp, Surface Sci. **140,** 275 (1984).
[13] S. Holloway, K. H. Benneman, Surface Sci. **101,** 327 (1980).
[14] M. P. Allen and D. J. Tildesley, Computer Simulation of Liquid, Clarendon Press, Oxford 1987.
[15] D. M. Heyes, J. Chem. Phys. **79,** 4010 (1983).
[16] Gy. I. Szász, K. Heinzinger, and W. O. Riede, Z. Naturforsch. **36a,** 1067 (1981).
[17] E. Spohr, G. Pálinkás, K. Heinzinger, P. Bopp, and M. M. Probst, J. Phys. Chem. **92,** 6754 (1988).